The Astronomical Journal, 136:2102–2106, 2008 November doi:10.1088/0004-6256/136/5/2102

A PROBABLE NEW GLOBULAR CLUSTER IN THE GALACTIC DISK

Jay Strader[1,3] and Henry A. Kobulnicky[2]
[1] Harvard-Smithsonian Center for Astrophysics, Cambridge, MA 02138, USA; jstrader@cfa.harvard.edu
[2] Department of Physics & Astronomy, University of Wyoming, 1000 E. University, Laramie, WY 82071, USA; chipk@uwyo.edu
Received 2008 July 10; accepted 2008 August 29; published 2008 October 13

ABSTRACT

We report the discovery of a probable new globular cluster (GC) in the disk of the Milky Way. Visible in the Two Micron All Sky Survey and the GLIMPSE Survey, it has an estimated foreground extinction of $A_V \sim 24$ mag. The absolute magnitude of the cluster and the luminosity function of the red giant branch are most consistent with that of an old GC with a mass of a few $\times 10^5\, M_\odot$ at a distance of 4–8 kpc.

Key words: galaxies: star clusters – globular clusters: general

Online-only material: color figure

1. INTRODUCTION

Harris (2001) estimated that there were ∼20 unknown Galactic globular clusters (GCs) hidden behind substantial foreground extinction in the disk or behind the bulge. Subsequent near-IR (NIR) surveys of the disk have borne out the prediction of missing clusters, two of which have been discovered in the Two Micron All Sky Survey (2MASS) by Hurt et al. (2000). Another cluster, GLIMPSE-C01, was found by Kobulnicky et al. (2005) using the *Spitzer*/IRAC GLIMPSE Survey (Benjamin et al. 2003) of the Galactic plane. The importance of the Galactic GC system in understanding the formation, evolution, and destruction of GCs motivates continuing efforts to finish the census of clusters.

In this paper, we report the discovery of a probable GC at Galactic coordinates $l = 14.13$, $b = -0.64$ (J2000 coordinates: $18^{\rm h}18^{\rm m}30^{\rm s} - 16^\circ58'36''$). This object was identified by Mercer et al. (2005) in a search for star clusters in GLIMPSE, although it was not suggested to be a GC. As this cluster is #3 in their catalog, we refer to the object as Mercer 3.

2. IMAGING

Figures 1 and 2 show 2MASS *JHK* images of a $2'.4 \times 2'.4$ area around Mercer 3, as well as a red Digitized Sky Survey (DSS) image on the same scale. The cluster is clearly visible in *H* and *K* but disappears in *J*, indicative of the high foreground reddening. There is no evidence of the cluster in the DSS image. In Figure 3, a composite color image of the Infrared Array Camera (IRAC) band 2 (4.5 μm), band 4 (8 μm), and MIPS 24 μm is shown. The morphology of the cluster is similar in the IRAC bands to that in *H* and *K*. Patchy, diffuse emission is visible across the frame. However, there is no evidence of a bubble or shell that could suggest a young cluster.

An elongated, opaque cloud dominates the composite image, located only $3'$ in projection from the cluster. Smaller dark clouds are located across the frame. We hypothesize that this large cloud complex is located in the foreground of the cluster and is the primary cause of the large extinction we derive later in the paper.

Using the 2MASS images, we performed integrated aperture photometry within a radius of $75''$ centered on the cluster, using a concentric sky aperture between $75''$ and $90''$. We do not claim that $75''$ is certain to be the edge of the cluster in a meaningful sense, but the extinction becomes noticeably variable at larger radii and so a larger aperture cannot be used. Thus, light in the outermost parts of the clusters will be lost. A competing effect is that our sky aperture may have larger extinction than the inner parts of the cluster, leading to an undersubtraction of the background and an overestimate of the cluster luminosity. It is difficult to assess the relative importance of these two effects and we caution the reader that our total magnitudes are likely to be uncertain at least at the 0.2–0.3 mag level.

We obtain total integrated magnitudes of $H = 7.3$ and $K = 6.1$ using the photometric calibration data in the headers of the 2MASS images and the equations listed in the 2MASS All-Sky Release documentation.[4] As a check on this calibration, we also downloaded and photometered the 2MASS *K*-band image of GLIMPSE-C01 from Kobulnicky et al. (2005), and found good agreement with the published *K* magnitude of the cluster.

The half-light radius of Mercer 3 in *K* is $\sim 39''$, but this is a lower limit due to the uncertainty in the amount of light at large radii and the extinction gradient in the image. For the likely distance range derived in Section 4, 4–8 kpc, this corresponds to a half-light radius between 0.8 and 1.5 pc. The low end of the range is smaller than nearly all Galactic GCs, while a value of 1.5 pc is smaller than typical, but not unusual. It is noteworthy that GLIMPSE-C01 and another recent Galactic plane discovery FSR 1767 (Bonatto et al. 2007) also have very small half-light radii of ∼0.6–0.7 pc (Kobulnicky et al. 2005; Bonatto & Bica 2008). It is unclear at present whether these small radii are accurate or are an artifact of the high extinction and the resultant difficulty in obtaining good surface brightness profiles.

3. STELLAR PHOTOMETRY

We used point source photometry taken from the Version 2.0 Data Release of GLIMPSE and matched it with 2MASS sources. Within a radius of $30''$ from the cluster center, we selected only those sources that are detected in all of *H*, *K*, and IRAC bands 1 and 2. Twenty-five stars fit these criteria. Figure 4 shows *K* versus $H - K$ and *K* versus $K - 3.6$ color–magnitude diagrams as observed; no extinction corrections have been applied. We

[3] Hubble Fellow.

[4] http://www.ipac.caltech.edu/2mass/releases/allsky/doc/explsup.html

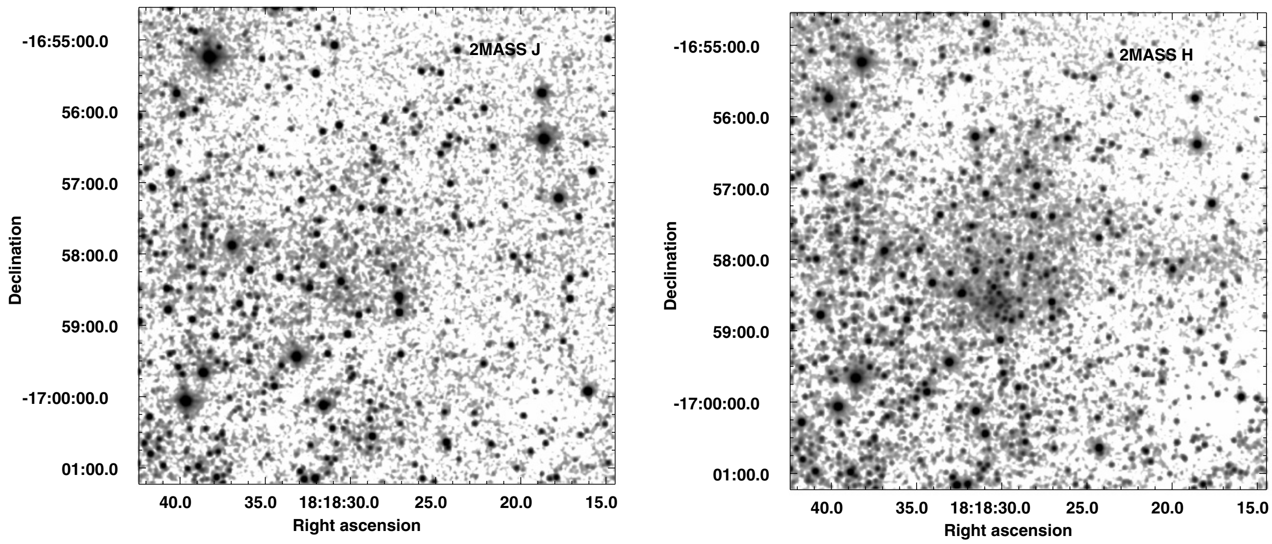

Figure 1. Postage stamp images of the cluster in 2MASS *JH*. The cluster is not visible in the *J* image due to high extinction.

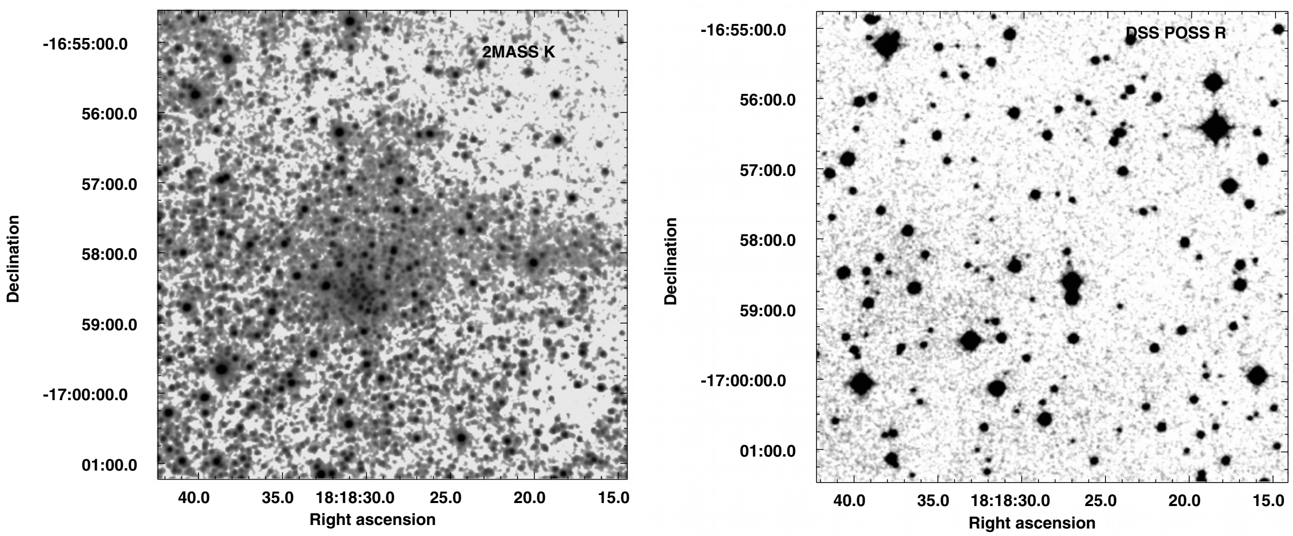

Figure 2. Postage stamp images of the cluster in 2MASS *K* and in red DSS. The cluster is not visible in DSS due to high extinction.

plotted 12 Gyr [M/H] $= -2$ isochrones from Marigo et al. (2008), assuming a distance of 5 kpc and $E(B-V) = 7.7$ (the values derived in Sections 3.1 and 4).

Both panels show a broad column of stars extending across $\sim$3 mag in K. The cutoff at $K \sim 14$ is due to the photometric limit of 2MASS; the IRAC images go somewhat deeper. A reasonable assumption is that these stars are the brightest red giants in the cluster, and that the spread in colors is due to differential extinction.

3.1. Extinction

We can constrain the extinction toward the cluster by noting the remarkable fact that the $H-K$ and $K-3.6$ colors of red giants vary little with age or metallicity, except at the tip of the red giant branch where there are few stars. While there are well-known relations between cluster metallicity and the NIR color of the red giant branch among Galactic GCs, these relations generally use $J-K$ or $J-H$ (e.g., Valenti et al. 2004), not $H-K$. Combining the Valenti et al. (2004) color-metallicity relations for $J-K$ and $J-H$ yields $H-K \propto 0.01$ [Fe/H] for $M_K \sim -3$ to -5. Inspection of the Marigo et al. (2008) isochrones for a wide range of ages and metallicities suggests that the typical spread in colors is no more than $\sim$0.1 mag in $H-K$ and 0.05 mag in $K-3.6$, which is consistent with the Valenti et al. empirical relationship (at least for old GCs). Thus, we can use a color–color plot to estimate the extinction with no knowledge of the metallicity or age of the cluster.

Figure 5 is a $K-3.6$ versus $H-K$ color–color plot. Overplotted are lines representing the reddened mean color of the upper red giant branch for a 12-Gyr-old GC; the isochrones used are from Marigo et al. (2008). Two extreme metallicities are plotted, -2 and 0. The reddenings range from $E(B-V) =$ 6 to 9, with crosses marking each magnitude of reddening. This figure shows that the unknown metallicity of the cluster has a minor effect on the color of the red giant branch compared to the spread in the points, suggesting that the differential extinction dominates the error. Since the lines do not pass directly through the center of the points, one derives a different reddening from each of the colors. In $H-K$ the mean reddening appears to be $E(B-V) \sim 7.8$, compared to $E(B-V) \sim 7.5$ for $K-3.6$. The differential reddening is at least 1 mag in both colors, though this may be exaggerated by the contamination of our sample with

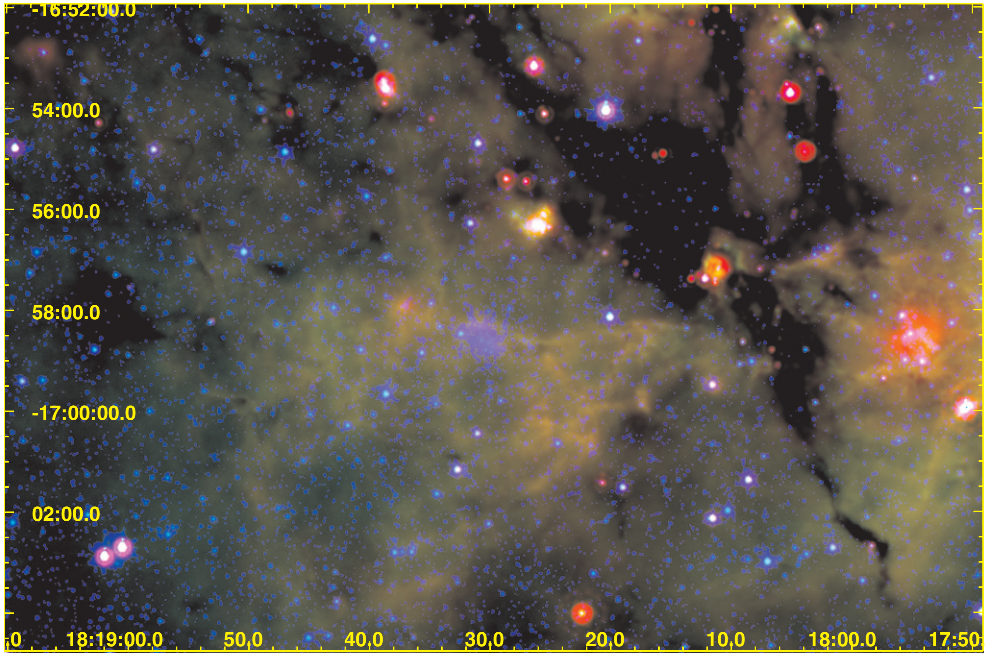

Figure 3. Three-color image using IRAC bands 2 and 4 and MIPS 24 μm, showing the cluster in the center of the image and its environment. Patchy extinction is present throughout the image, and a large infrared dark cloud is present only a few arcmin in projection from the cluster. This cloud may be associated with high extinction toward the cluster.

(A color version of this figure is available in the online journal.)

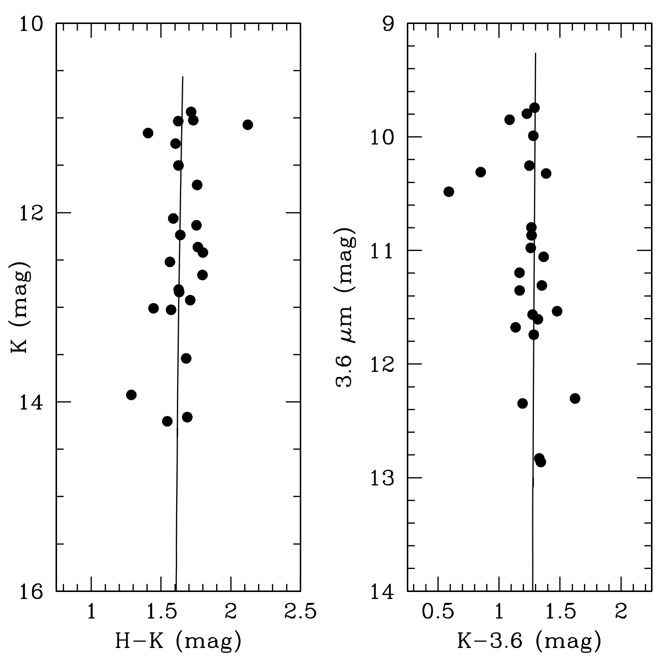

Figure 4. K vs. $H-K$ and 3.6 vs. $K-3.6$ color–magnitude diagrams of Mercer 3. 12 Gyr, [M/H] $= -2$ isochrones from Marigo et al. (2008) assuming $E(B-V) = 7.7$ and a distance of 5 kpc are overplotted.

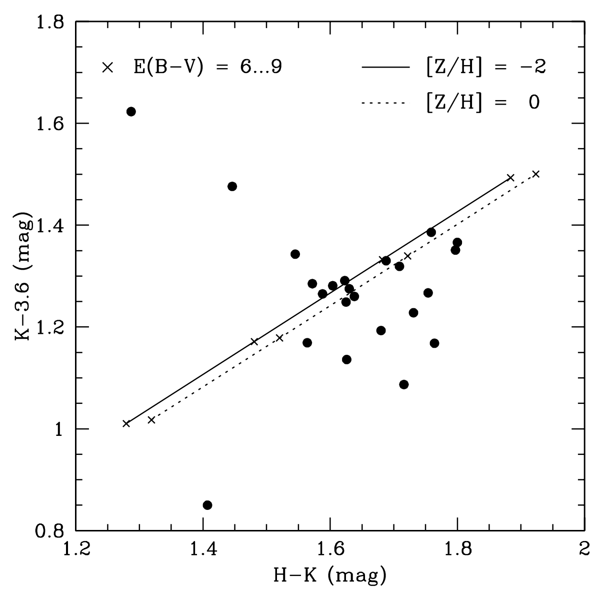

Figure 5. $K-3.6$ vs. $H-K$ color–color diagram of red giants in the cluster. Mean colors for the upper red giant branch using 12 Gyr isochrones with [M/H] $= -2$ (solid line) and 0 (dotted line) are overplotted; $E(B-V)$ ranges from 6 to 9 with crosses marking magnitude intervals. A value in the interval $7.5 \lesssim E(B-V) \lesssim 7.8$ is favored.

field stars (the stars lying far from the central clump in Figure 5, for example, are unlikely to be cluster members). Stellar population models are better tested in the classic NIR bands of H and K than in the newer *Spitzer* bands, so we tend to slightly favor the $H-K$ value. Thus we will adopt $E(B-V) \sim 7.7$ as our fiducial mean reddening, keeping in mind the presence of large differential reddening.

An $E(B-V)$ value of ~7.7 is extraordinarily high, corresponding to $A_K \sim 2.8$ and $A_V \sim 24$. We can do a sanity check by noting that the cluster is not detected in the 2MASS J image. The brightest red giants have $K \sim 11$, and are equivalent to an extincted $J \sim 16$. Below $J \sim 16$, especially in crowded regions, the completeness of 2MASS drops significantly, consistent with the absence of anything but a few stars at the position of the cluster in the J image in Figure 1. However, if the reddening were as low as $E(B-V) = 5.5$ or 6, then the brighter red giants would be visible in J. We conclude that our derived reddening is consistent with the lack of the cluster in the 2MASS J image.

3.2. *The Source of the Extinction*

As discussed above, Mercer 3 is located several arcmin in projection from a large IR dark cloud. It is possible that this cloud is associated with the material responsible for the large reddening toward the star cluster.

In their discovery paper of a GC in GLIMPSE, Kobulnicky et al. (2005) used relatively high-resolution CO data from the Galactic Ring Survey (Jackson et al. 2006) as a consistency check on the extinction toward their cluster. Unfortunately, Mercer 3 falls outside of the footprint of this survey, so we must fall back on older, lower-resolution data from the Massachusetts–Stony Brook Galactic Plane CO Survey (Clemens et al. 1986). The resolution of these data is $\sim 6'$, too low to compare the morphology of the cloud in Figure 3 to the CO maps.

We downloaded a data cube from this survey covering the position of our cluster and extracted an integrated CO spectrum at the position of our cluster. The only significant feature is a strong peak at 20 km s^{-1}. Integrating over the profile gives an intensity $I_{\rm CO} = 93$ K km s^{-1}. This may be converted into an H_2 column density and optical extinction using the equations in Bohlin et al. (1978; see also Kobulnicky & Skillman 2008): $N_{\rm H_2} = 3 \times 10^{20} I_{\rm CO}$ and

$$A_V = 3.1 \frac{2N_{\rm H_2}}{5.8 \times 10^{21}}. \quad (1)$$

Substitution yields $A_V \sim 30$ along this line of sight, which is generally consistent with the value derived from the color–color diagram. These equations assume that the CO is not optically thick and that there is no contribution of H I to the extinction, representing a lower limit. However, some of the molecular gas may be behind the cluster; due to the low resolution of the data, the gas might also be associated with a different cloud that is in front of the cluster but not contributing to the foreground extinction.

If we assume that the CO cloud is predominately in the foreground, then we can use its velocity to constrain the near/far distance of the cluster. For $v = 20$ km s^{-1} and a Galactic $l = 14.1$, the near/far distances are 2.4 and 14.1 kpc. We can take then, at the very least, 2.4 kpc as a lower limit on the cluster distance. In the following section we will use the color–magnitude diagram of cluster stars to derive an upper limit on the distance.

4. LUMINOSITY FUNCTION, AGE, AND DISTANCE

An additional constraint on the distance and age of the cluster comes from the stellar luminosity function (LF). With only 25 stars in the complete sample, creating a useful *K*-band LF is impractical. However, the GLIMPSE data are deeper, so if we relax the restriction on matches with 2MASS, we can select a sample of stars with detections in IRAC bands 1 and 2. Within $30''$ of the cluster center, there are 70 such stars. Figure 6 shows the 3.6 μm LF plotted as a density estimate, using an Epanechnikov kernel and a bin width of 0.25 mag. The main features of the LF are: (1) a lack of stars brighter than $m_{3.6} = 9$, (2) significant incompleteness below $m_{3.6} \sim 13$, and (3) a gently upward sloping LF between these two limits. Overplotted are theoretical LFs from Marigo et al. (2008) for solar metallicity and a range of ages from 1 Gyr to 12 Gyr (for old ages, the differences between metal-rich and metal-poor LFs in 3.6 μm are small compared to the quality of our data and the effect of differential reddening). These have been scaled in distance and normalization to produce the best match for each age.

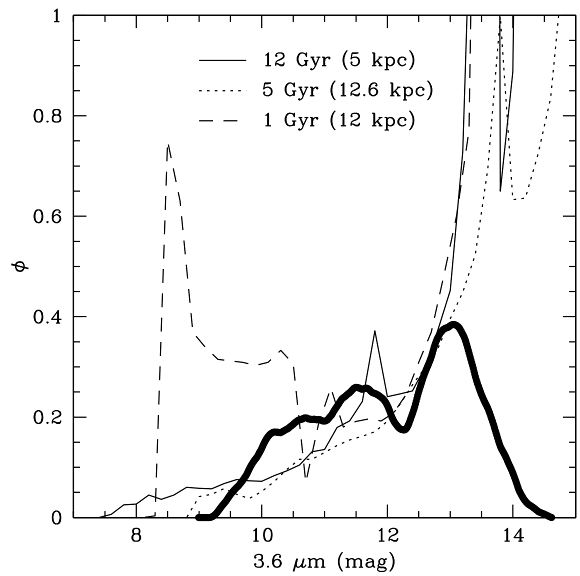

Figure 6. Observed 3.6 μm luminosity function compared to theoretical luminosity functions of solar metallicity from Marigo et al. (2008). These have ages of 12 Gyr (solid), 5 Gyr (dotted), and 1 Gyr (short dashed). Ages younger than a few Gyr are disfavored because of the lack of red supergiants.

A generic feature of the LFs for ages younger than $\sim$2–3 Gyr is a bump in the LF at the brightest magnitudes due to red supergiants. This bump is especially pronounced for ages of $\sim$1 Gyr and for certain younger ages. No such feature is seen in the observed LF. Thus, independent of the cluster distance, the LF is inconsistent with Mercer 3 being a young star cluster. The LF is most consistent with that of a relatively old open cluster or GC.

Further constraints on the distance of the cluster come from the assumption of a particular age. For a 12 Gyr solar metallicity stellar population, the maximum distance comes from identifying the brightest stars with the tip of the giant branch. This corresponds to an extincted distance modulus of $m - M \sim 16$, or $m - M_0 \sim 14.4$ using $A_{3.6} = 1.6$ (assuming $E(B - V) = 7.7$). Thus the maximal cluster distance is $\sim$7.6 kpc. The shape and normalization of the LF appear to be somewhat better fit by a distance of 5.0 kpc (this is the fit plotted in Figure 6), although the fit is far from perfect. Distances of 4 kpc or smaller are poor fits, as the theoretical LFs begin to rise steeply in a way that is unmatched by the data. This might partially be addressed by positing incompleteness at a brighter magnitude. Recall that the near-distance limit from the CO data was 2.4 kpc. We conclude that a plausible distance range for an old cluster is 4–8 kpc, with a value closer to the middle of that range being somewhat favored.

Assuming an age near the opposite extreme of the allowed range gives an upper limit on the distance. As shown in Figure 6, a 5 Gyr solar metallicity population appears to fit about as well as did the 12 Gyr LF. The implied distance is $\sim$12–13 kpc (with a large error). What does this long distance imply for the mass of the cluster? Given the extinction and total *K* magnitude discussed earlier, we derive $M_K \sim -12.1$ for a distance of 12 kpc. Using Maraston (2005) models with a Kroupa initial mass function, this is equivalent to a mass of $\sim 8 \times 10^5 M_\odot$. Mercer 3 would be one of the most massive star clusters in the Galaxy.

Alternatively, if we assume a distance of 5 kpc and an age of 12 Gyr, the implied mass is $\sim$2–3 $\times$ $10^5 M_\odot$ (depending on metallicity). This is close to the peak of the log-normal GC luminosity function and would essentially peg Mercer 3 as a typical Milky Way GC—keeping in mind that the total cluster luminosity is still quite uncertain.

As a conservative check on this mass estimate, we set aside the integrated K-band magnitude of the cluster for a moment and simply co-add the flux from all of the sources that lie along the red giant branch in Figure 4. This gives $K \sim 8.5$. We then make the almost absurd assumption that we have detected all of the red giants in the cluster (unlikely both because of incompleteness and because we are only considering sources within 30$''$ of the center). Noting that standard stellar population models (e.g., Worthey 1994) predict that 50–60% of the total K-band flux of an intermediate- to old-age object will be from the red giant branch, we derive a total K mag of $\sim$7.8. For an old object at 5 kpc, this corresponds to a mass of $\sim 5 \times 10^4 M_\odot$—less massive than a typical GC, but not unusual, and still much more massive than nearly all open clusters.

Our conclusion from this line of argument is that Mercer 3 is most likely to be a typical old GC, but we cannot rule out a less massive GC or a more massive intermediate-age object.

5. DISCUSSION

A secure identification of Mercer 3 as an old GC will require moderately deep NIR photometry. The predicted main sequence turnoff is at $K \sim 19$. If, instead, it is a massive intermediate-age cluster, the turnoff would be significantly fainter: for the Figure 6 fiducial case of a 5 Gyr cluster at 12.6 kpc, the predicted turnoff is at $K \sim 20.5$ (this is a combination of the cluster being $\sim$2 mag more distant but with a turnoff $\sim$0.5 mag more luminous). The shape of the subgiant branch would also be different between old and intermediate-age clusters. Due to the large and differential reddening, an accurate estimate of the cluster metallicity will probably require NIR spectroscopy. This is easily accomplished as the brightest red giants have $K \sim 11$.

Mercer 3 is the second probable GC discovered using *Spitzer* and 2MASS; a further two GCs were found using 2MASS alone. At the opposite end of parameter space, Koposov et al. (2007) discovered two extraordinarily low-mass GCs in the Sloan Digital Sky Survey at heliocentric distances of $\sim$40–50 kpc. The continuing pace of these discoveries suggests that the Galactic cluster census is far from complete.

J.S. was supported by NASA through a Hubble Fellowship, administered by STScI. We thank Dan Clemens, Laura Chomiuk, and Beth Willman for useful comments on the manuscript. The paper was improved by the suggestions of an anonymous referee.

Note added in manuscript. While this manuscript was under review, a paper by Kurtev et al. (2008) appeared on arXiv.org, reporting a contemporaneous discovery of this cluster. These authors arrive at very similar conclusions regarding the distance, extinction, and age of the cluster.

REFERENCES

Benjamin, R. A., et al. 2003, PASP, 115, 953
Bohlin, R. C., Savage, B. D., & Drake, J. F. 1978, ApJ, 224, 132
Bonatto, C., & Bica, E. 2008, A&A, 479, 741
Bonatto, C., Bica, E., Ortolani, S., & Barbuy, B. 2007, MNRAS, 381, L45
Clemens, D. P., Sanders, D. B., Scoville, N. Z., & Solomon, P. M. 1986, ApJS, 60, 297
Harris, W. E. 2001, in Star Clusters, Saas-Fee Advanced Course 28, ed. L. Labbardt, & B. Binggeli (Berlin: Springer), 223
Hurt, R. L., Jarrett, T. H., Kirkpatrick, J. D., Cutri, R. M., Schneider, S. E., Skrutskie, M., & van Driel, W. 2000, AJ, 120, 1876
Jackson, J. M., et al. 2006, ApJS, 163, 145
Kobulnicky, H. A., & Skillman, E. D. 2008, AJ, 135, 527
Kobulnicky, H. A., et al. 2005, AJ, 129, 239
Koposov, S., et al. 2007, ApJ, 669, 337
Kurtev, R., Ivanov, V., Borissova, J., & Ortolani, S. 2008, A&A, 489, 583
Maraston, C. 2005, MNRAS, 362, 799
Marigo, P., Girardi, L., Bressan, A., Groenewegen, M. A. T., Silva, L., & Granato, G. L. 2008, A&A, 482, 883
Mercer, E. P., et al. 2005, ApJ, 635, 560
Valenti, E., Ferraro, F. R., & Origlia, L. 2004, MNRAS, 351, 1204
Worthey, G. 1994, ApJS, 95, 107